CHAPTER 180

NUMERICAL MODELING OF DISPERSION IN STRATIFIED WATERS

by

George C. Christodoulou[1]

Jerome J. Connor[2]

ABSTRACT

A numerical model is developed for the quantitative description of the dispersion process in a two-layer system which represents an approximation for a natural coastal water body during the summer season when a distinct thermocline usually exists. The formulation is based on the convection-diffusion equation, vertically integrated between the layer boundaries. Layer velocities and thicknesses are assumed to be obtained from a separate hydrodynamic model. The quantification of the physical processes of entrainment and mixing through the density interface as well as the horizontal dispersion mechanisms is discussed.

The finite element method is chosen for numerical implementation because of its flexibility in grid layout and easier handling of spatial and temporal variability. Triangular elements with linear interpolation functions are used for the spatial discretization, while a simple implicit iterative scheme based on the trapezoidal rule is employed for time integration. The method is shown to be unconditionally stable, for an arbitrary grid and both one- and two-layer problems, when there is no iteration and the parameters are constant. General convergence criteria required by the iteration procedure are developed and expressed in terms of the basic parameters of the problem and are subsequently confirmed by numerical experiments. Verification of the model is performed by comparison with analytical solutions derived for counterflow conditions. Finally the model is applied to a particle dispersion experiment carried out recently in the Massachusetts Bay and comparisons with field data are presented.

---

[1]Research Assistant, Ralph M. Parsons Laboratory for Water Resources and Hydrodynamics, M.I.T., Cambridge, Mass., U.S.A.

[2]Professor of Civil Engineering, Department of Civil Engineering, M.I.T., Cambridge, Mass., U.S.A.

INTRODUCTION

Coastal dispersion problems have received considerable attention in recent years, due to the rapid growth in the development of the coastal zone and the increasing concern for the impact on the coastal environment. Mathematical models of the hydrodynamic processes involved have been developed in the past based on the assumption that flow parameters and concentrations are approximately uniform over the water column, resulting in a depth-averaged treatment of the problem. This approach is justified to some extent by the characteristic shallow-ness of coastal water bodies, as compared to their horizontal dimensions. However, the assumption of uniformity is no longer valid during the summer season, when a significant stratification usually exists.

The presence of a strong thermocline suggests the idealization of the flow field as a two-layer system. This is the simplest stratified case and it is felt that it has to be studied prior to proceeding to a multilayer approach, for understanding the fundamental physical behavior of dispersion in a layered system. Multilayer or quasi-three dimensional models of the transport of constituents are presently being incorporated into large multipurpose computer codes [1, 8, 9] utilizing finite difference techniques. Such models will require difficult and costly verification studies and extensive field data (especially boundary conditions) for their proper application to a given area. A simpler two-layer model needs less "tuning" and is much more economical, while still providing a good approximation to the actual conditions when a distinct thermocline exists.

In this paper, problems associated with properly describing the dispersion of matter in a two-layer system are investigated. First, the mathematical formulation is presented and the modeling of the physical processes involved is discussed. Then, the details of the finite element method are examined and, in particular, its stability requirements in this class of problems are established. Lastly, the applicability of the numerical model to real world problems is addressed.

MATHEMATICAL FORMULATION

The present model is intended to describe the dispersion of an arbitrary constituent, possessing vertical mobility, in a two-layer coastal water body of variable bottom topography and boundary geometry. The velocity field in both layers as well as the layer thicknesses will be assumed known, presumably

obtainable through a separate hydrodynamic model. By uncoupling the hydrodynamic and dispersion models, the same flow pattern can be used to investigate very economically the spreading of several different substances and to experiment with different source locations, loading strategies, parameter values, etc. However, this can only be done provided that the constituent of interest does not affect significantly the flow field or the density structure.

The mass balance of a constituent is expressed by the 3-D convection-diffusion equation:

$$\frac{\partial c}{\partial t} = - \frac{\partial}{\partial x}(uc+q_x) - \frac{\partial}{\partial y}(vc+q_y) - \frac{\partial}{\partial z}((w-w_s)c+q_z) + p \qquad (1)$$

where

  u, v, w are the water velocities in the x,y,z directions

  w_s is the particle settling velocity, positive downward

  q_x, q_y, q_z are diffusive fluxes in the x,y,z directions

  p represents generation or decay of the constituent

Integrating between the layer boundaries (Figure 1) and using Leibnitz's rule, one obtains for the top layer

$$\frac{\partial}{\partial t}\int_{-h_1}^{\eta} c\,dz = - \frac{\partial}{\partial x}\int_{-h_1}^{\eta}(uc+q_x)dz - \frac{\partial}{\partial x}\int_{-h_1}^{\eta}(vc+q_y) + \int_{-b_1}^{\eta} p\,dz$$

$$+[c(\frac{D\eta}{Dt} - w+w_s)-q_s]_\eta + [c(\frac{Dh_1}{Dt}+w-w_s)-q_i]_{-h_1}$$
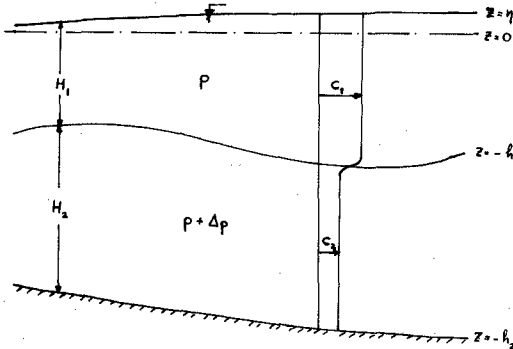

Figure 1: The Two-Layer Idealization

The terms in brackets represent fluxes through the free surface and interface, respectively. The kinematic condition at the surface requires

$$[\frac{D\eta}{Dt} - w]_\eta = 0$$

However, the interface, defined as the position of steepest density gradient, is not necessarily a material surface. We may write in general

$$[w + \frac{Dh_1}{Dt}]_{-h_1} = w_e$$

and refer to the relative velocity, w_e, of the water particles with respect to the layer boundary as "entrainment" velocity. This is considered positive when directed upward, indicating net water motion from the bottom to the top layer. The other component, q_i, of the interfacial transport is a diffusive flux and can be expressed in terms of the difference in concentration between the layers. Approximating the concentration at the interface as the average value of the two layers, the overall transfer is expressed as:

$$Q_{21} = (w_e - w_s)c_{-h_1} - q_i = (w_e - w_s)\frac{c_1 + c_2}{2} + \alpha(c_2 - c_1) \qquad (2)$$

In large water bodies, the erosion of the quiescent lower layer by the upper layer, moving under the influence of wind or other driving mechanism, is explained by the one-way transport of water toward the turbulent layer. In coastal areas, both layers are quite turbulent and possess velocities of the same order of magnitude, hence water exchange both ways through the interface should be anticipated. Denoting the respective volumetric rates per unit area by m_{21} and m_{12} (Figure 2), the net transfer of material is:

$$Q_{21} = m_{21}c_2 - m_{12}c_1 \qquad (3)$$

By comparing Equations (2) and (3) it is evident that

$$w_e = m_{21} - m_{12} \qquad (4a)$$

$$\alpha = (m_{21} + m_{12})/2 \qquad (4b)$$

Several experimental and theoretical investigations in 1-D two-layer systems have been carried out in the past mostly with one layer quiescent, as reviewed in [3, 15, 11]. The one-way rate of transport, usually measured by the thickening of the moving layer, has been expressed with different velocity and length scales so that at first only a qualitative agreement between them is evident. Upon careful examination, however, it may be seen [5] that a rather general expression in terms of the mean flow characteristics can be given, as follows:

$$m_{ji} = \frac{10^{-3} U_i}{Ri_o} \qquad i,j = 1,2 \qquad (5)$$

where the overall Richardson number for a 2-D flow is defined as

$$Ri_o = \frac{g \frac{\Delta\rho}{\rho} H}{(\vec{U}_i - \vec{U}_j)^2}$$

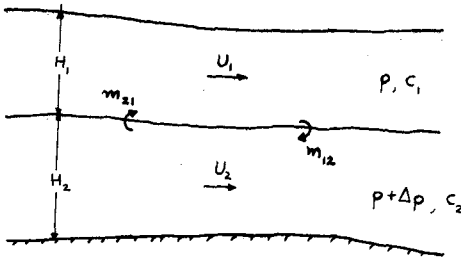where H is the average layer thickness, i.e., half the depth.

Figure 2: Schematization of Interfacial Transport

We introduce now the following notation

$$C_1 = \int_{-h_1}^{\eta} c\,dz = \bar{c}_1 H_1$$

$u = \bar{u}+u''$, $v = \bar{v}+v''$, $c = \bar{c}+c''$

where the overbar denotes layer average value and the double prime spatial deviation from that average. Then, Equation 2 takes the form

$$\frac{\partial C_1}{\partial t} + \frac{\partial}{\partial x}(\bar{u}_1 C_1) + \frac{\partial}{\partial y}(\bar{v}_1 C_1) = -\frac{\partial}{\partial x} Q_{x_1} - \frac{\partial}{\partial y} Q_{y_1} + P_1 \qquad (6)$$

where P_1 includes source, decay and interfacial flux terms, and the total dispersive fluxes Q_{x_1}, Q_{y_1} are approximated as follows:

$$Q_{x_1} = -\int_{-h_1}^{\eta} (u''c''+q_x)dz = H_1(E_{xx_1}\frac{\partial \bar{c}_1}{\partial x} + E_{xy_1}\frac{\partial \bar{c}_1}{\partial y}) \qquad (7a)$$

$$Q_{y_1} = \int_{-h_1}^{\eta} (v''c''+q_y)dz = H_1(E_{yx_1}\frac{\partial \bar{c}_1}{\partial x} + E_{yy_1}\frac{\partial \bar{c}_1}{\partial y}) \qquad (7b)$$

The dispersion coefficients

$$\underset{\sim}{E} = [\begin{array}{cc} E_{xx} & E_{xy} \\ E_{yx} & E_{yy} \end{array}] = \underset{\sim}{E}^d + \underset{\sim}{\varepsilon}$$

comprise a second order tensor consisting of a shear-dispersion part and an eddy diffusivity part. The analogy of the effective horizontal spreading due to nonuniformity of the velocity profile to the turbulent diffusion process has

been shown initially by G.I. Taylor [14] for flow through a pipe and later
by Elder [7] for flow in an open channel. By extending their arguments to the
case where both u and v velocity components are present, one may prove the
validity of Eqs.(7a, b) with shear dispersion coefficients given by [5]:

$$E_{xx}^d = \frac{1}{H} \int_0^H \frac{1}{\varepsilon_x} [\int_0^H u''d\zeta]^2 dz \tag{8a}$$

$$E_{yy}^d = \frac{1}{H} \int_0^H \frac{1}{\varepsilon_z} [\int_0^H v''d\zeta]^2 dz \tag{8b}$$

$$E_{xy}^d = E_{yx}^d = \frac{1}{H} \int_0^H \frac{1}{\varepsilon_z} [\int_0^H u''d\zeta][\int_0^H v''d\zeta]dz \tag{8c}$$

where ε_z is the vertical eddy diffusion coefficient.

The horizontal turbulent diffusion term accounts for mixing due to horizontal
eddies. Based on the theory of locally isotropic turbulence, the well-known
4/3 law is derived. According to [12]

$$\varepsilon = b \ e^{1/3} \ L^{4/3} \tag{9}$$

where

  e is the rate of energy input

  L is a length scale and

  b is a numerical constant of order 0.1.

As the cloud size increases, larger scale motions are being incorporated
into the diffusion term, explaining the length dependence of the diffusion
coefficient. It should be clear, however, that this depends on the detail
of specification of the advection processes. In the case that the velocity
field is specified at certain grid points and the cloud increases beyond the
level of discretization, internal mixing is now (partly) described by the
advection terms, and hence the length scale of Equation (3) should be related
to the grid size.

An alternative expression for ε, based on mixing length arguments, is
[2,6]:

$$\varepsilon = L^2\sqrt{\phi} \tag{10}$$

where

$$\phi = 2(\frac{\partial \bar{u}}{\partial x})^2 + 2(\frac{\partial \bar{v}}{\partial y})^2 + (\frac{\partial \bar{u}}{\partial y} + \frac{\partial \bar{v}}{\partial x})^2$$

This has the advantage of using the readily available mean velocity gradients
instead of the energy input. According to [6], the sub-grid scale eddy
coefficient is modeled by a length scale an order of magnitude smaller than

the grid size. However, the resolution of the flow field description associated with spatial averaging in the hydrodynamic model employed has to be taken into account and the coefficient increased accordingly.

THE FINITE ELEMENT METHOD

For each layer, the governing equation has the form (6). The boundary conditions are (Figure 3)

1) Essential, i.e., the concentration is specified on the boundary segment S_c: $C = C*$

2) Natural, i.e., the normal concentration gradient, or, equivantly, the normal dispersion flux, is specified on the boundary segment S_q:
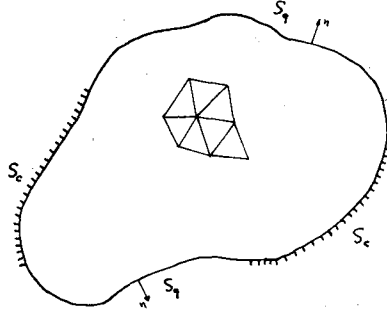
$Q_n = Q_n^*$

Figure 3: Solution Field and Boundary Conditions

In seeking an approximate solution, the partial differential equation and the flux boundary condition are multiplied by a weighting function (w) and the residual R over the domain is required to vanish:

$$R = \iint_A \{\frac{\partial C}{\partial t} + \frac{\partial (\bar{u}C)}{\partial x} + \frac{\partial (\bar{v}C)}{\partial y} + \frac{\partial}{\partial x} Q_x + \frac{\partial}{\partial y} Q_y - P\} \, wdA +$$

$$+ \int_{S_q} (Q_n^* - Q_n)wdS = 0 \tag{11}$$

Employing partial integration, this is rewritten as

$$R = \iint_A [\{\frac{\partial C}{\partial t} + \frac{\partial}{\partial x}(\bar{u}C) + \frac{\partial}{\partial y}(\bar{v}C) - P\}w - Q_x \frac{\partial w}{\partial x} - Q_y \frac{\partial w}{\partial y}] \, dA$$

$$+ \int_{S_q} Q_n^* wdS = 0 \tag{12}$$

It should be mentioned that the trial function C is required to satisfy the essential boundary condition and the weighting function to satisfy the homogeneous form, i.e., $w = 0$ on S_c.

Expression (12) is called the symmetrical weak form and involves only first derivatives of both trial and test functions, which can therefore be chosen from the same solution space. In the finite element method the domain is subdivided into elements and the total residual is evaluated as the sum of element residuals. By introducing interpolation functions within each element, the continuous problem is transformed to a discrete one, with the concentrations at the nodal points as unknowns. Triangular elements with linear interpolation functions are used herein, as in the one layer model [10]. Setting

$$C = \underset{\sim}{N} C^e \qquad w = \Delta C = \underset{\sim}{N} \Delta C^e$$

the element residual becomes:

$$R^e = (\Delta C^e)^T (\underset{\sim}{M}^e \frac{dC^e}{dt} - \underset{\sim}{P}^e) + (\Delta C^e)^T \underset{\sim}{F}^{be} \tag{13}$$

where

$$\underset{\sim}{M}^e = \iint_{A^e} \underset{\sim}{N}^T \underset{\sim}{N} \, dA \tag{14a}$$

$$\underset{\sim}{P}^e = \iint_{A^e} [\underset{\sim}{N}^T (P - \frac{\partial}{\partial x}(\bar{u}C) - \frac{\partial}{\partial y}(\bar{u}C) + \frac{\partial \underset{\sim}{N}^T}{\partial x} Q_x + \frac{\partial \underset{\sim}{N}^T}{\partial y} Q_y] dA \tag{14b}$$

$$\underset{\sim}{F}^{be} = \int_{S_q^e} \underset{\sim}{N}^{bT} Q_n^* dS \tag{14c}$$

Carrying out the summation over all elements for each layer results in:

$$R = \sum_e R^e = (\Delta C)^T (\underset{\sim}{M}\dot{C} - \underset{\sim}{P} + \underset{\sim}{F}^b) = 0$$

and since ΔC is arbitrary,

$$\underset{\sim}{M}C = \underset{\sim}{P} - \underset{\sim}{F}^b = \underset{\sim}{\hat{P}} \tag{15}$$

This constitutes a set of linear ordinary differential equations and is integrated by using an implicit iterative trapezoidal scheme, as follows:

$$C_{1,t+\Delta t}^{(i+1)} = C_{1,t} + \frac{\Delta t}{2} \underset{\sim}{M}^{-1} (\hat{P}_{1,t+\Delta t}^{(i)} + \hat{P}_{1,t}) \tag{16a}$$

$$C_{2,t+\Delta t}^{(i+1)} = C_{2,t} + \frac{\Delta t}{2} \underset{\sim}{M}^{-1} (\hat{P}_{2,t+\Delta t}^{(i)} + \hat{P}_{2,t}) \tag{16b}$$

Since the geometrical matrix $\underset{\sim}{M}$ is time-invariant it has to be inverted only once. By lumping all other terms in the $\underset{\sim}{\hat{P}}$ vector, maximum flexibility in handling time variability of any or all of the relevant parameters and loadings is achieved. In addition, any non-linear relations of the various terms to the concentrations can be readily handled in this way. In practice, the iteration

continues until either the change in concentration between current and previous values is below a specified tolerance or the number of iterations reaches an imposed upper limit.

STABILITY ANALYSIS

Expanding the $\hat{\underset{\sim}{P}}$ vector leads to the following form of the matrix equation for each layer

$$\underset{\sim\sim}{M}\dot{\underset{\sim}{C}} + \underset{\sim\sim}{A}\underset{\sim}{C} + \underset{\sim\sim}{K}\underset{\sim}{C} + \underset{\sim}{D}\underset{\sim}{C} = \underset{\sim}{S} \tag{17}$$

where $\underset{\sim}{A}$ is associated with advection, $\underset{\sim}{K}$ with dispersion, $\underset{\sim}{D}$ with decay and $\underset{\sim}{S}$ includes sources and boundary conditions. The trapezoidal integration rule is expressed as follows

$$[\underset{\sim}{M} + \frac{\Delta t}{2}(\underset{\sim}{A}+\underset{\sim}{K}+\underset{\sim}{D})_{n+1}]\underset{\sim}{C}_{n+1} = [\underset{\sim}{M} - \frac{\Delta t}{2}(\underset{\sim}{A}+\underset{\sim}{K}+\underset{\sim}{D})_n]\underset{\sim}{C}_n$$

$$+ \frac{\Delta t}{2}(\underset{\sim}{S}_n + \underset{\sim}{S}_{n+1}) \tag{18}$$

To investigate the stability of the scheme, we consider the homogeneous case, i.e., $\underset{\sim}{S}_n = \underset{\sim}{S}_{n+1} = 0$, and assume the various matrices are constant over the time step. We note that the geometrical, decay, and dispersion matrices, being composed of individual symmetric positive definite sub-matrices, also have these properties. Continuity considerationa and the compatibility of inter-element velocity expansions [5], leads to:

$$\underset{\sim\sim}{A}\underset{\sim}{C} = - \underset{\sim}{A}^T\underset{\sim}{C} + \int_{S_q} u_n \underset{\sim}{N}^{bT} \underset{\sim}{N}^b \, dS \, \underset{\sim}{C}^b \tag{19}$$

where the superscript b denotes boundary quantity and u_n is the velocity normal to the boundary (positive outwards). Writing the advection matrix as the sum of a symmetric and a skew-symmetric part

$$\underset{\sim}{A} = \underset{\sim s}{A} + \underset{\sim ss}{A}$$

it is seen that the former usually vaniahes since normally S_q refers to land boundaries where the normal velocity is zero.

By writing

$$\underset{\sim}{C}_{n+1} = \underset{\sim}{a} \, \underset{\sim}{C}_n \tag{20}$$

where a is the amplification matrix, one may set

$$\underset{\sim}{C}_n = \lambda^n \, \underset{\sim}{\Phi} \tag{21}$$

where λ is an eigenvalue of $\underset{\sim}{a}$.

The necessary condition for stability is

$$||\underset{\sim}{a}|| < 1 \text{ or } |\lambda| < 1$$

Substituting (21) into the homogeneous form of (18), premultiplying by $\underset{\sim}{\Phi}^T$ and noting that, according to the above discussion

$$\underset{\sim}{\Phi}^T \underset{\sim}{M} \underset{\sim}{\Phi} = m > 0$$
$$\underset{\sim}{\Phi}^T \underset{\sim}{K} \underset{\sim}{\Phi} = \kappa > 0$$
$$\underset{\sim}{\Phi}^T \underset{\sim}{D} \underset{\sim}{\Phi} = d > 0$$
$$\underset{\sim}{\Phi}^T \underset{\sim}{A} \underset{\sim}{\Phi} = ia_{ss}$$

we obtain for λ

$$\lambda \{m + \frac{\Delta t}{2} (\kappa + d + ia_{ss})\} = m - \frac{\Delta t}{2} (\kappa + d + ia_{ss})$$

or,

$$\lambda^2 = \frac{[m - \frac{\Delta t}{2} (\kappa + d)]^2 + a_{ss}^2}{[m + \frac{\Delta t}{2}(\kappa + d)]^2 + a_{ss}^2} < 1 \tag{22}$$

This indicates that the scheme is unconditionally stable for an arbitrary grid.

However, the time step is always limited by the desired detail of description of the time variability of inputs or parameters of the problem. When the matrices $\underset{\sim}{K}$, $\underset{\sim}{D}$, $\underset{\sim}{A}$ are actually variable, it becomes uneconomical to form and invert matrices of the form $\underset{\sim}{M} + \frac{\Delta t}{2} (\underset{\sim}{A} + \underset{\sim}{K} + \underset{\sim}{D})$ every time-step. This is a basic reason for resorting to the iteration procedure discussed earlier, which may be written in expanded form:

$$\underset{\sim}{M} C_{n+1}^{(i+1)} = [\underset{\sim}{M} - \frac{\Delta t}{2}(\underset{\sim}{A}+\underset{\sim}{K}+\underset{\sim}{D})_n] C_n - \frac{\Delta t}{2}(\underset{\sim}{A}+\underset{\sim}{K}+\underset{\sim}{D})_{n+1} C_{n+1}^{(i)} \tag{23}$$

For convergence of the iteration, however, a restriction on the time step is required. The general sufficient condition

$$||\underset{\sim}{M}^{-1} \frac{\Delta t}{2} (\underset{\sim}{A}+\underset{\sim}{K}+\underset{\sim}{D})|| < 1 \tag{24}$$

leads to

$$\Delta t < \frac{2}{||\underset{\sim}{M}^{-1}(\underset{\sim}{A}+\underset{\sim}{K}+\underset{\sim}{D})||}$$

or, the more restrictive condition:

$$\Delta t < \frac{2}{||\underset{\sim}{M}^{-1}\underset{\sim}{A}|| + ||\underset{\sim}{M}^{-1}\underset{\sim}{K}|| + ||\underset{\sim}{M}^{-1}\underset{\sim}{D}||} \tag{25}$$

Unfortunately, (25) is not practical in this form, since one does not have an explicit relation between the time step and the parameters of the problem. An approximation to it can be obtained by considering a single element only, forming the matrices and evaluating their norms, i.e., their eigenvalues. For uniform velocity U, isotropic dispersion E and decay rate k, the resulting expression for an equilateral triangle of size Δs is [5]:

$$\Delta t < \frac{1}{\frac{\sqrt{3}}{2} \frac{U}{\Delta s} + \frac{8E}{\Delta s^2} + \frac{k}{2}} \tag{26}$$

This was obtained using the average eigenvalue of the $\underset{\sim}{M}^{-1}\underset{\sim}{K}$ matrix. The same result is arrived at for a right triangle, when the flow is parallel to one of the legs of the right angle, of size Δs. The conclusions reached at the element level can be conservatively generalized for the whole domain, provided the "worst case" element is considered.

A similar analysis for the two-layer problem shows that the time integration scheme is again unconditionally stable, with no iteration. The latter requires a restriction on the time step analogous to (25). Another term has now to be added in the denominator to account for interfacial mixing, i.e., $||\underset{\sim}{M}^{-1}\underset{\sim}{E}||$. Evaluating this term for a single triangle results in the addition of $\alpha'/2$ in the denominator of (26), where α' is the interfacial mixing rate normalized by the layer thicknesses. This term is usually small and consequently the time step is essentially governed by the "worst" layer.

Experimental confirmation of condition (26) was attempted by means of test runs carried out in the 1-D grid shown in Figure 5. The contribution of the decay term was of the order of 1% and thus neglected. For each run, a point was plotted on the plane of the non-dimensional coordinates ($U\Delta t/\Delta s$, $E\Delta t/\Delta s^2$). These points are shown in Figure 4 along with the theoretical bound (26). The symbols used are defined in Table 1. It is seen that runs corresponding to points within the "safe" area always converge well, while outside the theoretical boundary more or less significant errors are present, eventually leading to instability a little further outside. Further, the line $E/U\Delta s = 1/2$ is seen to exactly separate runs with and without significant upstream negatives and spatial oscillations due to the approximation of steep concentration gradients. This condition, analogous to finite difference schemes, was derived theoretically [5] and earlier empirically [10]. Thus, accuracy considerations actually reduce the acceptable area to a fraction of the safe region for iteration convergence. Additional runs, carried out in 2-D test grids, as well as grids of natural water bodies, compiled in [5], show the theoretical limit to be still approximately valid.

VERIFICATION AND APPLICATIONS

To test the correctness of the model structure, comparisons with analytical solutions are desirable. However, the availability of analytical solutions is restricted to very simple flow conditions. In Figure 6, the numerical model is compared with the solution for an instantaneous point source in the top layer of a 1-D counterflow. A unit load is distributed between the three nodes at $x = 0$
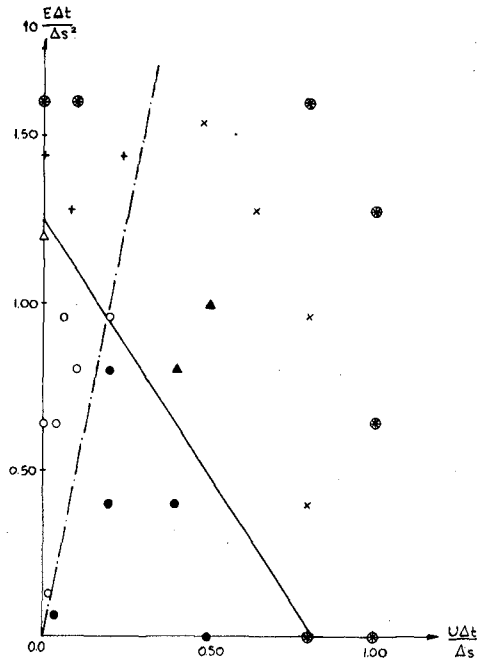
Figure 4   Comparison of Theoretical Bound on the Time Step with 1-D Runs

Table 1

Definition of Symbols used in Figure 4

Symbol	Error after 10 Iterations	Negatives as Percent of Peak	Remarks
0	< 1%	< 10%	Good, smooth solution
●	< 1%	> 10%	Iteration converges well, but result exhibits oscillations
Δ	< 10%	< 10%	Iteration error goes down rapidly as time proceeds
▲	< 10%	> 10%	
+	> 10%	< 10%	It. Error does not always decrease rapidly (some may eventually blow up)
x	> 10%	> 10%	
⊕	—	—	Blows up

of the grid of Figure 5, and the results adjusted to yield values per unit width
of the channel. A unit depth is assumed for each layer. Zero concentration is
specified at the ends of the grid and zero flux is prescribed along the side
boundaries. The parameters used are

$$U_1 = -U_2 = 0.05 \text{ m/sec}$$
$$E_1 = E_2 = 0.01 \text{ m}^2/\text{sec}$$
$$\alpha = 5 \times 10^{-4} \text{ m/sec}$$
$$\kappa = 0$$

It may be observed from Figure 6 that the lower layer concentrations are two
orders of magnitude smaller than those of the top layer. This supports to some
extent the treatment of the interface as a barrier. However, it may not hold
for longer time periods and is certainly not valid for substances possessing
vertical mobility. Irrespective of that, it should be clear that a great advantage
of the two-layer treatment is the more detailed description of the velocity field.
In this particular counterflow case the depth-average velocity is zero, implying
a stationary peak of the depth-averaged concentration distribution located at
the origin. As shown in Figure 6, this is far from the actual depth-averaged
concentration distribution of the two-layer system. Further verification studies
can be found in [5].

     To establish confidence in the predictive capability of the model and the
degree of its applicability under natural conditions, further verification,
consisting of comparisons to real-world cases, is necessary. For this purpose a
dispersion experiment was carried out by M.I.T., sponsored by the Boston Edison
Co., in the vicinity of the Pilgrim Nuclear Power Station (PNPS) on the
Massachusetts coast (Figure 7) in August 1975. Five hundred pounds of small
fluorescent sphalerite (ZnS) particles were introduced into the water and
their motion subsequently monitored for 5 days by boat and by helicopter.
Also, two current meter stations had been installed prior to the experiment as
indicated in Figure 7 by dots.

     The finite element grid used was the same as in the previous applications of
one-layer models to the Bay. The value of the dispersion coefficient, 30 m^2/sec,
and the difference in tidal amplitude between the ends of the open boundary, were
kept the same as established for the one-layer models [13]. The circulation model
used to obtain velocity inputs is that of Wang and Connor [16]. Since it requires
both layers to extend over the whole domain, some nodal depths had to be increased
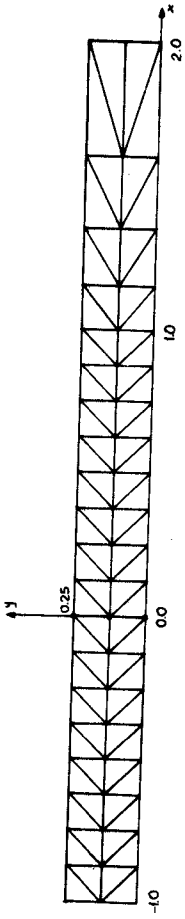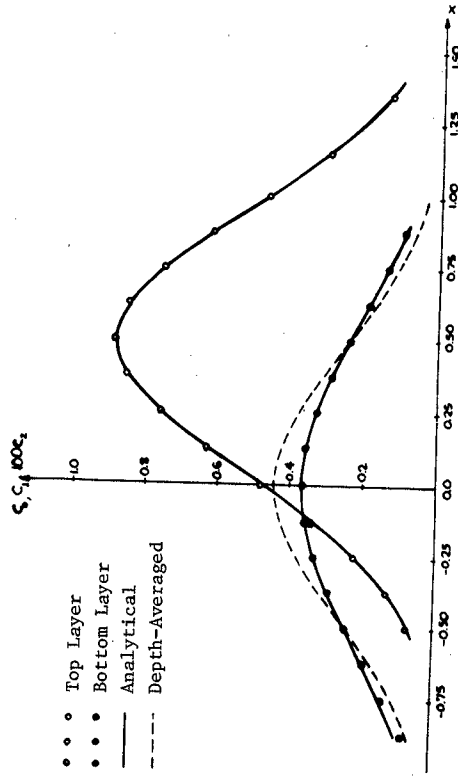
Figure 5 One-dimensional Finite Element Test Grid

Figure 6 1-D Distribution at t=10 sec. after an Instantaneous Injection

to at least 15 m in order to avoid intersection of the interface with the bottom.
The position of the interface was set at 8 meters as initial condition, consistent
with available information [4].   However, much more detailed data are needed for
the specification of interface motion along the ocean boundary.   In view of
lack of such data at present, the interface was assumed to be linear along the
boundary and various cases, e.g. remaining fixed over the tidal cycle or
moving with the same amplitude as the free surface, were examined.   Actual
time-varying wind data were used in the computations.
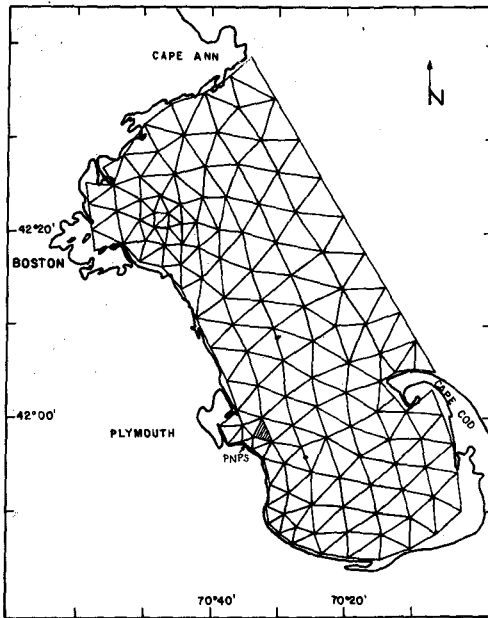

Figure 7   Mass. Bay Finite Element Grid and
           Location of the MIT Experiment

The experimental results were reduced to layer-average concentrations by averaging together samples taken above and below the thermocline to yield a single representative value for each layer. The resulting plots, in particles/lt, are shown in Figures 8 and 9 corresponding to 2 and 3 days after the dumping took place. The plume is seen to move slowly to the southeast, approximately parallel to the shore and later extending to the east.

In the dispersion simulations the shaded triangle was loaded over a period of three timesteps. The area of the triangle is quite large in comparison to the actual source and as a consequence one should expect unrealistically large plume areas for short times. The interfacial mixing rate is set at 10^{-5} m/sec and the settling velocity at 7.3×10^{-5} m/sec, based on an average particle size of 7 microns. The computed concentrations 2 and 3 days after the injection are shown in Figures 10 and 11. Taking into account the initial spreading of the source, good qualitative agreement with respect to the size and location of the plume as well as the peak values is observed.

CONCLUSION

The objective of this study was to investigate the problem of dispersion in coastal water bodies under conditions of strong stratification. The two-layer idealization was adopted as a useful extreme case and, at the same time, the easiest to handle mathematically. The ability of the two-layer treatment to handle transport between the layers is important, whether or not the constituent of interest has some vertical mobility, in providing a refined picture of the distribution over the depth. A further advantage of the two-layer formulation, evident from both ideal and real-world applications, lies in the more detailed description of the velocity field. However, the sensitivity of the results to variations in the flow field points out the necessity for using realistic current input.

Additional fundamental research is needed for better understanding the turbulent mixing processes in stratified environments. Also, field monitoring programs are required to provide reliable inputs, primarily on the behavior of the interface along open boundaries of the domain under consideration. It is believed that the present two-layer model, providing an extreme-case picture of the response of the physical system, can be a useful tool in coastal dispersion studies.
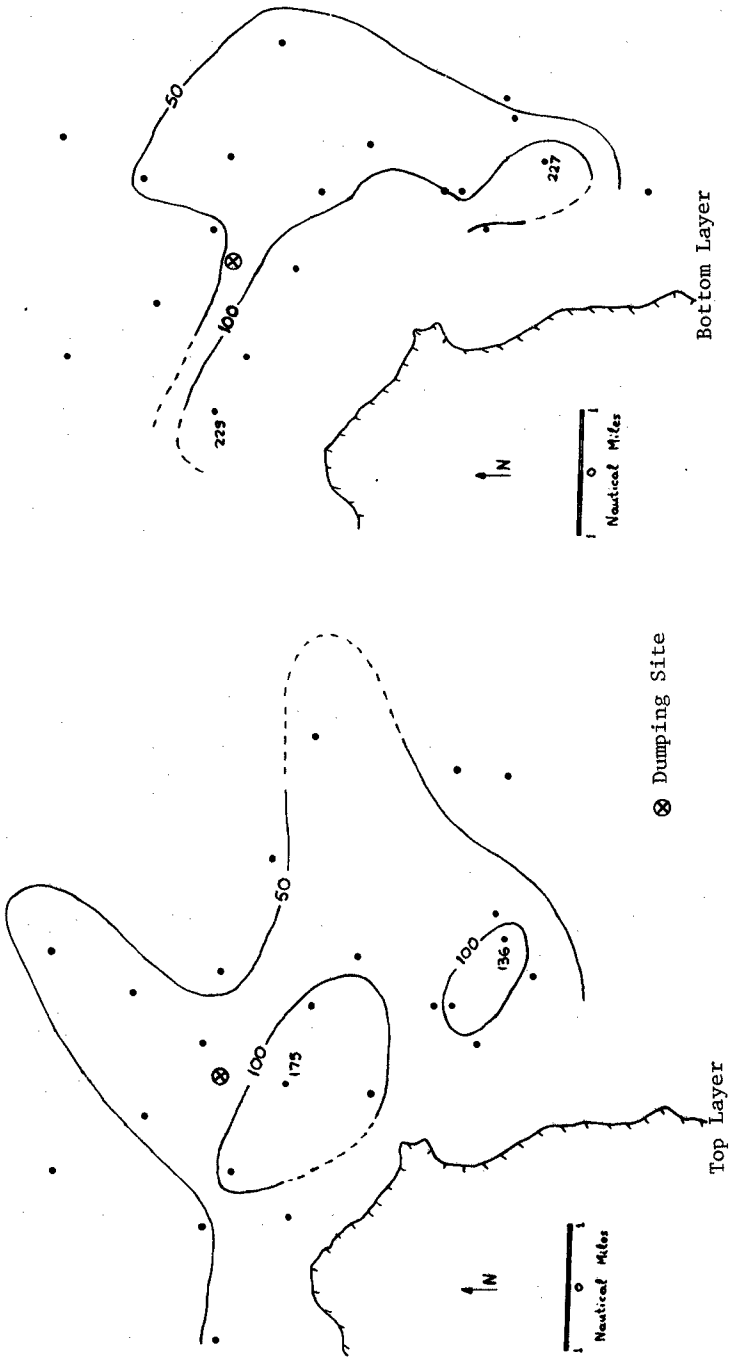
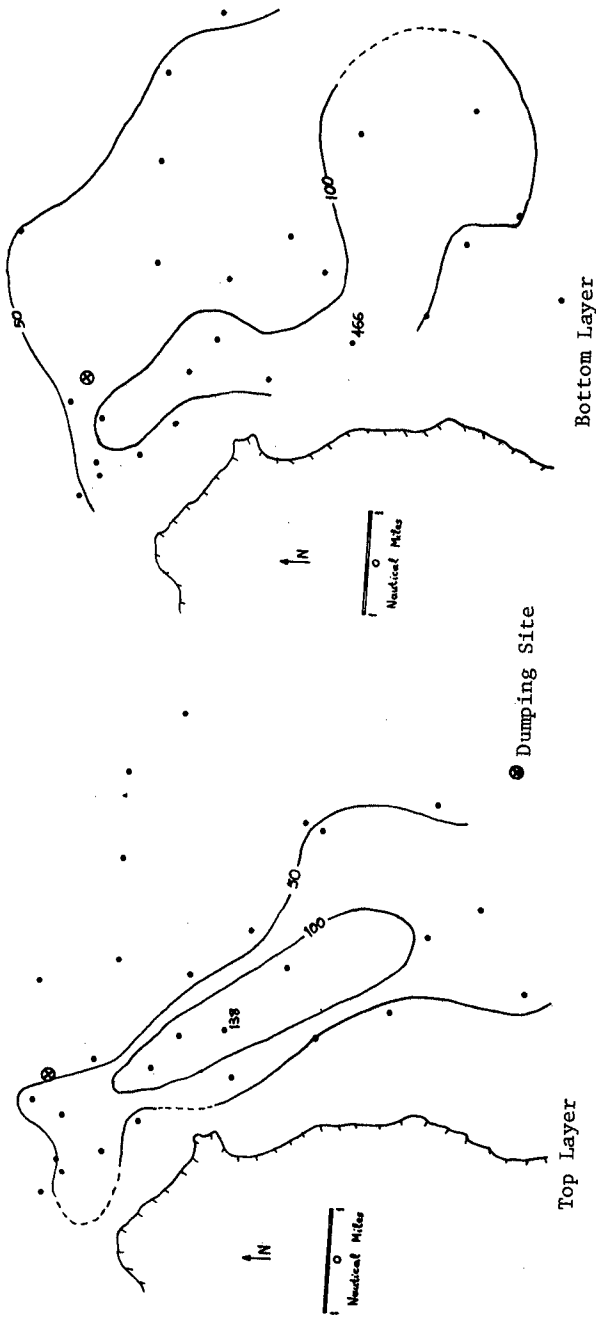Figure 8   Experimental Results at Day D+2

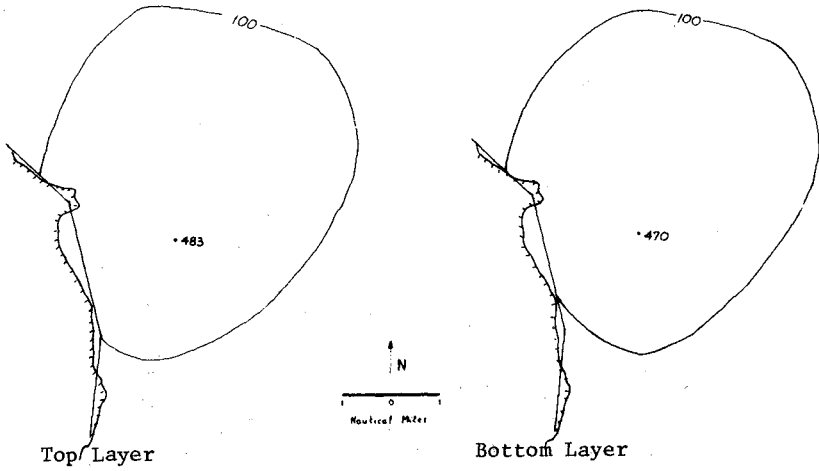Figure 9 Experimental Results at Day D+3

Top Layer   Bottom Layer

Figure 10   Computed Concentrations at Day D+2

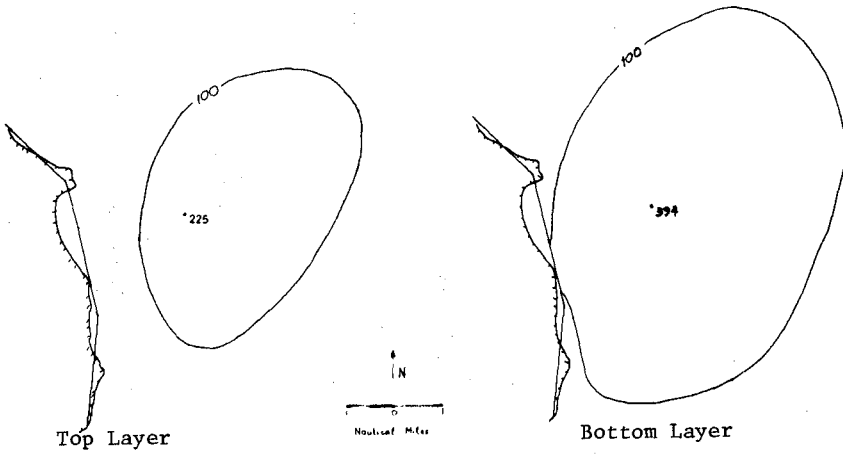Top Layer   Bottom Layer

Figure 11   Computed Concentrations at Day D+3

REFERENCES

1. Abbott, M.B. et al, " Systems Modeling of Stratified Fluids", Symposium
    on Modeling Techniques 'Modeling 75', San Francisco, September 1975

2. Boericke, R.R. and Hall, D.W., "Hydraulic and Thermal Dispersion in an
    Irregular Estuary", J. Hydraulics Div., ASCE, Vol. 100, HY1, January 1974

3. Breusers, H.N.C. (ed.), "Momentum and Mass Transfer in Stratified Flows",
    Literature Study, Delft Hydraulics Lab Report R880, December 1974

4. Bumpus, D.F., "Review of the Physical Oceanography of Massachusetts Bay",
    Woods Hole Oceanographic Inst. Report 74-8, February 1974

5. Christodoulou, G.C., "Mathematical Modeling of Dispersion in Stratified
    Waters", Sc.D. Thesis, Dept. of Civil Engineering, M.I.T., September 1976

6. Deardorff, J.W., "On the Magnitude of the Subgrid Scale Eddy Coefficient",
    J. Computational Physics, Vol. 7, Part 1, 1971

7. Elder, J.W., "The Dispersion of Marked Fluid in Turbulent Shear Flow",
    J. Fluid Mechanics, Vol. 5, Part 4, May 1959

8. Laevastu, T., "Multilayer Hydrodynamical Numerical Models", Symposium on
    Modeling Techniques 'Modeling 75', San Francisco, September 1975

9. Leendertse, J.J. and Liu, S.K., "A Three-Dimensional Model for Estuaries
    and Coastal Seas: Vol. II, Aspects of Computation", Rand Co., June 1975

10. Leimkuhler, W.F. et al, "Two-Dimensional Finite Element Dispersion Model",
    Symposium on Modeling Techniques 'Modeling 75', San Francisco, September 1975

11. Long, R.R., "The Influence of Shear on Mixing Across Density Interfaces",
    J. Fluid Mechanics, Vol. 70, Part 2, July 1975

12. Osmidov, R.V., "On the Turbulent Exchange in a Stably Stratified Ocean",
    Izv. Acad. of Science USSR, Atmospheric and Oceanic Physics, Vol. 1, No. 8, 1965

13. Pearce, B.R. and Christodoulou, C.C., "Application of a Finite Element Dispersion
    Model for Coastal Waters", Proceedings of XVI I.A.H.R. Congress, Sao Paulo, 1975

14. Taylor, C.I., "The Dispersion of Matter in Turbulent Flow through a Pipe", Proc.
    Royal Society of London, Ser. A, Vol. 223, 1954

15. Turner, J.S., "Buoyancy Effects in Fluids", Cambridge Univ. Press, 1973

16. Wang, J.D. and Connor, J.J., "Finite Element Model of Two Layer Coastal
    Circulation", Proceedings of XIV International Coastal Engineering Conference,
    Copenhagen, 1974